RSC Advances

PAPER

View Article Online
View Journal | View Issue

Check for updates

Cite this: *RSC Adv.*, 2018, **8**, 33710

Lu^{3+} doping induced photoluminescence enhancement in novel high-efficiency $Ba_3Eu(BO_3)_3$ red phosphors for near-UV-excited warm-white LEDs

Bin Li, G. Annadurai, Jia Liang, Liangling Sun, Shaoying Wang, Qi Sun and Xiaoyong Huang *

$Ba_3Eu(BO_3)_3$ (BEB) and Lu^{3+} doped BEB red phosphors were successfully synthesized by a high-temperature solid-state reaction method. X-ray diffraction (XRD) patterns, excitation and emission spectra, decay lifetimes, CIE coordinates, internal quantum efficiency, and thermal stability of these phosphors were systematically studied. Under 395 nm excitation, these phosphors exhibited high-brightness red emissions centred at 611 nm. In addition, it was found that doping appropriate amounts of Lu^{3+} ions into BEB phosphors can improve their photoluminescence intensity and internal quantum efficiency. The integrated emission intensity of BEB:0.3Lu^{3+} phosphor was about 1.34 times that of BEB phosphor. Compared with commercial red phosphor $Y_2O_2S:Eu^{3+}$, BEB:0.3Lu^{3+} phosphor showed better color purity (91.4%) and higher emission intensity (about 3.25 times). Surprisingly, the BEB:0.3Lu^{3+} phosphor had a high internal quantum efficiency of almost 87%, which was higher than that of 83% for BEB phosphors. Meanwhile, the BEB:0.3Lu^{3+} phosphors also exhibited good thermal stability with activation energy around 0.14 eV, and the integrated emission intensity at 423 K remained about 52% of that at 303 K. Finally, by using commercial $BaMgAl_{10}O_{17}:Eu^{2+}$ blue phosphors, commercial $(Ba,Sr)_2SiO_4:Eu^{2+}$ green phosphors, as-prepared BEB:0.3Lu^{3+} red phosphors and a 395 nm near-ultraviolet-emitting light-emitting diode (LED) chip, a prototype warm white LED device was fabricated, which showed good color rendering index (CRI = 84.7) and low correlated color temperature (CCT = 3377 K).

Received 28th August 2018
Accepted 25th September 2018

DOI: 10.1039/c8ra07166g

rsc.li/rsc-advances

Open Access Article. Published on 02 October 2018. Downloaded on 2/10/2026 8:09:48 AM.
This article is licensed under a Creative Commons Attribution-NonCommercial 3.0 Unported Licence.

Introduction

Over the past decades, inorganic luminescent materials with outstanding optical properties have been extensively investigated because of their promising applications in a variety of fields, such as white light emitting diodes (WLEDs), fluorescent lamps, multicolor displays, solar cells, sensors, plant growth, and bioimaging.[1–8] Among of them, red-emitting phosphors, as the supplement of red light for white light emitting diodes (WLEDs), are commonly used to improve the inefficient performance of commercial WLEDs. This type of WLED, which was fabricated using a blue chip coated with yellow $Y_3Al_5O_{12}:Ce^{3+}$ phosphor, suffered from low color rendering index (CRI < 70) and high correlated color temperature (CCT > 7000),[9–15] due to the deficiency of a red component.[16–20] Recently, a new type of WLED emerged, which was fabricated by using red, green, and blue (RGB) phosphors and the near ultraviolet (NUV) chips, because its CRI as well as CCT were improved tremendously (CRI > 80 and CCT < 6000).[21–23] As the red candidate component in this new type of WLED, Eu^{3+} ion-based inorganic red phosphors were extensively investigated because of the bright red light emission arising from the $^5D_0 \rightarrow {}^7F_2$ transition of Eu^{3+} ions.[24,25] However, different hosts would influence the performance of Eu^{3+},[26–36] such as internal quantum efficiency, photoluminescence thermal stability, and color purity.[7,18,37]

Borates are good hosts for making phosphors have been broad applied in lighting and displays field due to their low synthesis temperature, good chemical stability and various crystal structures.[38–41] In this work, we investigated the photoluminescence properties of a red-emitting host, $Ba_3Eu(BO_3)_3$ (BEB), which belongs to trigonal structure with space group $R\bar{3}$, and its cell parameters $a = 13.071$ Å, $b = 13.071$ Å, $c = 9.563$ Å.[42] In addition, we doped Lu^{3+} ions into the Eu^{3+} ions sites to enhance the photoluminescence of red emitting BEB:xLu^{3+} ($x = 0$, 0.1, 0.3, 0.5, 0.7, 0.9) phosphors. By characterizing XRD, PL and PLE spectrum as well as decay lifetime of these phosphors, we found that substituting part of Eu^{3+} ions by Lu^{3+} can enhance the photoluminescence intensity, decay lifetimes and internal quantum

College of Physics and Optoelectronics, Taiyuan University of Technology, Taiyuan 030024, P. R. China. E-mail: huangxy04@126.com

This journal is © The Royal Society of Chemistry 2018

Open Access Article. Published on 02 October 2018. Downloaded on 2/10/2026 8:09:48 AM.
This article is licensed under a Creative Commons Attribution-NonCommercial 3.0 Unported Licence.

efficiency of BEB phosphor. Surprisingly, the optimal phosphor BEB:0.3Lu^{3+} presented better internal quantum efficiency (IQE: 87%) than some other reported red phosphors, such as $Na_3Sc_2(PO_4)_3$:0.35Eu^{3+} (IQE: 49%) and $MBaY_{1-x}Eu_x(BO_3)_2$ (IQE: 48%).[11,23] Moreover, the phosphors possessed good thermal stability (the photoluminescence intensity at 423 K was about 52% of that at 303 K). Finally, for investigating the application of the red emitting BEB:xEu^{3+} phosphors, we made a fabricated prototype warm WLED device by coating our red BEB:0.3Lu^{3+}, commercial blue $BaMgAl_{10}O_{17}$:Eu^{2+} (BAM:Eu^{2+}) and green $(Ba,Sr)_2SiO_4$:Eu^{2+} phosphors on a 395 nm-emitting (NUV) chip.[43,44]

Experimental

A series of BEB:xLu^{3+} (x = 0, 0.1, 0.3, 0.5, 0.7, 0.9, and 1.0) samples were successfully synthesized *via* a conventional high-temperature solid-state reaction. H_3BO_3 (99.9%), $BaCO_3$ (99.9%), Lu_2O_3 (99.99%), and Eu_2O_3 (99.99%) were used as raw materials. According to the stoichiometric ratio, these raw materials were weighed and ground in an agate mortar to achieve uniformity. In order to compensate the volatilization, the amount of H_3BO_3 was in excess of 5 wt%. Then these uniform mixtures were put in the alumina crucibles and sintered at 1373 K for 4 h. After that, the furnace cooled down naturally to room temperature, and the final products were ground and collected for further characterization.

The X-ray diffraction (XRD) patterns of the phosphors were recorded on a Bruker D8 X-ray diffractometer by using Cu Kα radiation ranging with 10–80° at step rate of 0.02°. The room-temperature photoluminescence emission (PL) and photoluminescence excitation (PLE) spectra and luminescence decay lifetimes of phosphors were measured by Edinburgh FS5 spectrometer equipped with a 150 W continued- and pulsed-wavelength xenon lamps. Temperature-dependent PL spectra were recorded by using same spectrophotometer and detectors equipped with a temperature controller. The internal quantum efficiency (IQE) of the samples was measured on an Edinburgh FS5 spectrometer equipped with an integrating sphere coated with $BaSO_4$.

The commercial blue BAM:Eu^{2+}, green $(Ba,Sr)_2SiO_4$:Eu^{2+}, and our red BEB:0.3Lu^{3+} phosphors were mixed with silicone thoroughly, and the obtained phosphor–silicone mixture was coated on the surface of the LED chips to fabricate WLED device. The photoelectric properties of the fabricated devices were measured by using an integrating sphere spectroradiometer system (HAAS2000, Everfine). WLEDs were operated at 3 V with various drive currents of 20, 60, 120, 180, 240, and 300 mA, respectively. The spectral power distributions of WLEDs were measured using a corrected spectrometer to calculate their values of CCT and CRI.

Results and discussion

Phase formation

The XRD patterns of BEB:xLu^{3+} (x = 0, 0.1, 0.3, 0.5, 0.7, 0.9, and 1.0) were presented in the Fig. 1. As can be seen, the XRD profiles of samples were not all corresponding to one critical

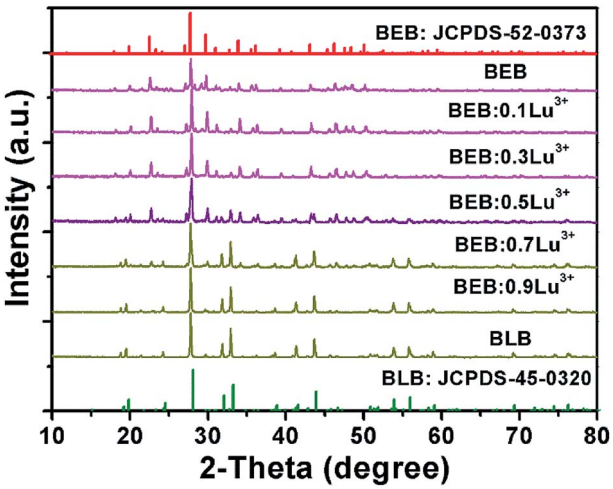

Fig. 1 XRD patterns of BEB:xLu^{3+} (x = 0, 0.1, 0.3, 0.5, 0.7, 0.9, and 1.0) phosphors. The standard data of BLB (JCPDS-45-0320) and BEB (JCPDS-52-0373) were shown.

JCPDS card. Interestingly, the crystal phase of phosphors were divided into two groups and changed from BEB (JCPDS-52-0373) to $Ba_3Lu(BO_3)_3$ (BLB) (JCPDS-45-0320) upon increasing the concentration of Lu^{3+} ions. The phosphors (x < 0.5) were coincided with BEB phase, whereas other phosphors (x > 0.5) were consistent with BLB phase. However, the two phases were co-existent in BEB:0.5Lu^{3+} sample by comparing its XRD peaks with the above two JCPDS cards. It is suggests that the BEB:0.5Lu^{3+} phosphor was a mixed phase compound. Accordingly, the explanation for above result is the difference of ionic radius of Eu^{3+} (0.947 Å) and Lu^{3+} (0.861 Å).[45] Owing to the fact that Eu^{3+} ions were replaced by smaller Lu^{3+} ions, the crystal space group changed from $R\bar{3}$ (148) of BEB to $P6_3cm$ (185) of BLB.[42]

Luminescence properties of BEB:xLu^{3+}

In order to investigate the photoluminescence properties of Eu^{3+}, the PLE and PL spectra of BEB:xLu^{3+} (x = 0, 0.1, 0.3, 0.5, 0.7, 0.9) phosphors were recorded and shown in the Fig. 2. As presented in the Fig. 2(a), the PLE spectra of phosphors had same profiles, although they belonged to two different phase. It can be clearly seen that several sharp peaks centered at 323 nm ($^7F_0 \rightarrow {}^5H_J$ transition), and 363 nm ($^7F_0 \rightarrow {}^5D_4$ transition), 384 nm ($^7F_0 \rightarrow {}^5G_J$ transition), 395 nm ($^7F_0 \rightarrow {}^5L_6$ transition), 415 nm ($^7F_0 \rightarrow {}^5D_3$ transition), 465 nm ($^7F_0 \rightarrow {}^5D_2$ transition), and 527 nm ($^7F_0 \rightarrow {}^5D_1$ transition).[46–51] However, there were some differences on PL spectra, which were described in Fig. 2(b). Under excited at 395 nm, all phosphors presented a series of characteristic emissions, which located at 590 nm ($^5D_0 \rightarrow {}^7F_1$ transition), 611 nm ($^5D_0 \rightarrow {}^7F_2$ transition), 656 nm ($^5D_0 \rightarrow {}^7F_3$ transition), and 705 nm ($^5D_0 \rightarrow {}^7F_4$ transition).[11,52–56] However, with doping Lu^{3+} ions into BEB, the PL intensity increased until x = 0.3 (the intensity of BEB:0.3Lu^{3+} was almost 1.34 times of that of BEB), and then dropped rashly after doping Lu^{3+} ions heavily. The results can be explained by the concentration quenching of Eu^{3+} ions. In other words, doping Lu^{3+}

Open Access Article. Published on 02 October 2018. Downloaded on 2/10/2026 8:09:48 AM.
This article is licensed under a Creative Commons Attribution-NonCommercial 3.0 Unported Licence.

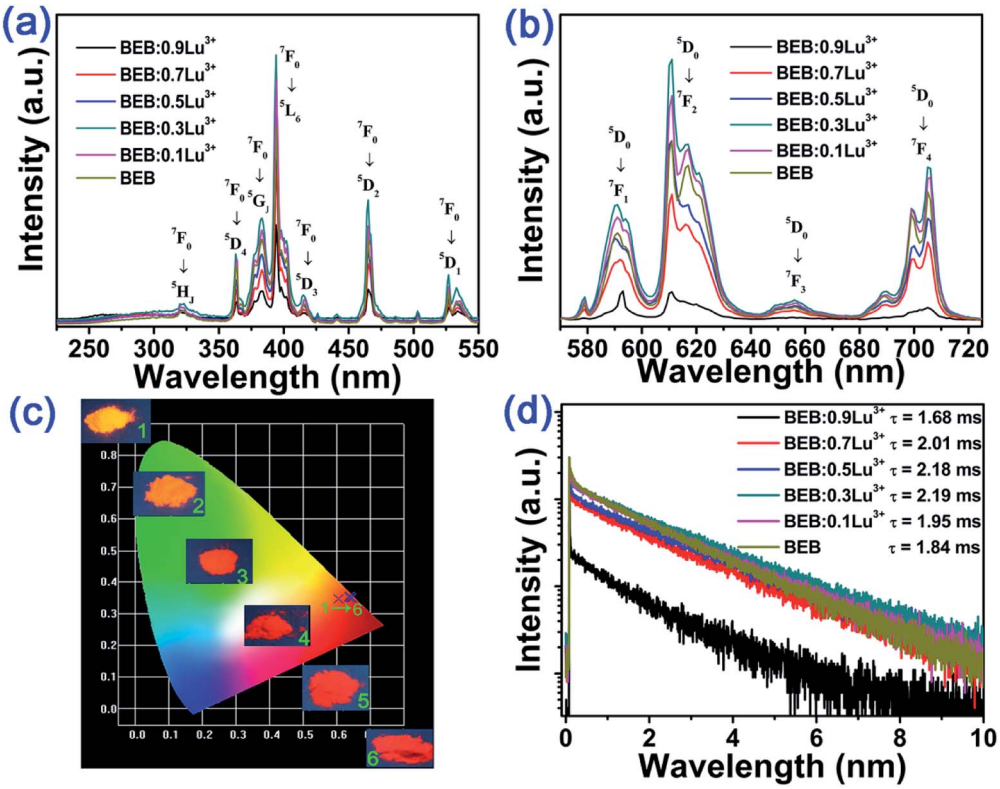

Fig. 2 (a) PLE spectra and (b) PL spectra of BEB:xLu^{3+} (x = 0, 0.1, 0.2, 0.3, 0.5, 0.7, and 0.9) phosphors. (c) Digital photographs BEB:xLu^{3+} phosphors with different Lu^{3+} contents (1: x = 0.9; 2: x = 0.7; 3: x = 0.5; 4: x = 0.3; 5: x = 0.1; and 6: x = 0). (d) Photoluminescence lifetimes of BEB:xLu^{3+} phosphors.

ions in BEB host can alleviate the concentration quenching and enlarge the distance of two adjacent Eu^{3+} ions. The distance (hereafter abbreviated as R_c) can be calculated by the following formula:[37]

$$R_c = 2\left[\frac{3V}{4\pi CN}\right]^{1/3} \quad (1)$$

where C is the concentration of Eu^{3+} ions, N is number of available crystallographic sites occupied by the activator ions in the unit cell, and V is the cell volume. For the BEB host, the V, C and N were 1415 Å^3, 1, and 7, respectively. Accordingly, the R_c of BEB host was determined to be 7.28 Å, while the R_c of BEB:0.3Lu^{3+} was calculated to be about 8.20 Å. Studied by Dexter, stretching the distance between two adjacent Eu^{3+} ions through doping Lu^{3+} ions can reduce the possibility of cross relaxation ($^5D_1 + {}^7F_0 = {}^5D_0 + {}^7F_3$) between two neighboring Eu^{3+} ions.[57,58] Therefore, doping Lu^{3+} ions to increase the distance between Eu^{3+} ions can be regarded as a great method to enhance PL intensity of BEB phosphor.

Interestingly, the emission color of BEB:xLu^{3+} phosphors can also be influenced by the concentration of Lu^{3+}. As shown in Fig. 2(c), the emission colors of phosphors under a 365 nm UV lamp changed from red to orange by increasing Lu^{3+} ions content. Furthermore, the calculated coordinate value (x, y) of the Commission Internationale de L'Eclairage (CIE) and R/O values for the ratio of red to orange, which symbolized the ratio of $^5D_0 \rightarrow {}^7F_2$ to $^5D_0 \rightarrow {}^7F_1$, were listed in Table 1. Similarly, CIE coordinates for the phosphors shifted apparently from orange to red (sample 1 (BEB:0.9Lu^{3+}) to sample 6 (BEB), shown in Fig. 2(c)). This phenomenon is due to the different transitions of $^5D_0 \rightarrow {}^7F_1$ and $^5D_0 \rightarrow {}^7F_2$, which can generate orange and red emissions, respectively. Therefore, the R/O value could affect the CIE coordinates of phosphors.

The decay curves of all phosphors were also recorded and demonstrated in Fig. 2(d). The fluorescence average lifetimes τ can be obtained by the following formula:[21,29]

$$I(t) = I\exp(-t/\tau) \quad (2)$$

where I refers to intensities, and τ represents the corresponding decay time for the exponential components, respectively. The obtained decay lifetimes of $^5D_0 \rightarrow {}^7F_2$ transition were

Table 1 The comparisons of different properties for BEB:xLu^{3+} phosphors

BEB:xLu^{3+}	R/O	CIE (x, y)	IQEs
x = 0	2.55	(0.644, 0.351)	~83%
x = 0.1	2.41	(0.642, 0.353)	~84%
x = 0.3	2.29	(0.640, 0.354)	~87%
x = 0.5	2.21	(0.638, 0.356)	~75%
x = 0.7	2.06	(0.638, 0.353)	~66%
x = 0.9	1.85	(0.604, 0.348)	~57%

This journal is © The Royal Society of Chemistry 2018

Open Access Article. Published on 02 October 2018. Downloaded on 2/10/2026 8:09:48 AM.
This article is licensed under a Creative Commons Attribution-NonCommercial 3.0 Unported Licence.

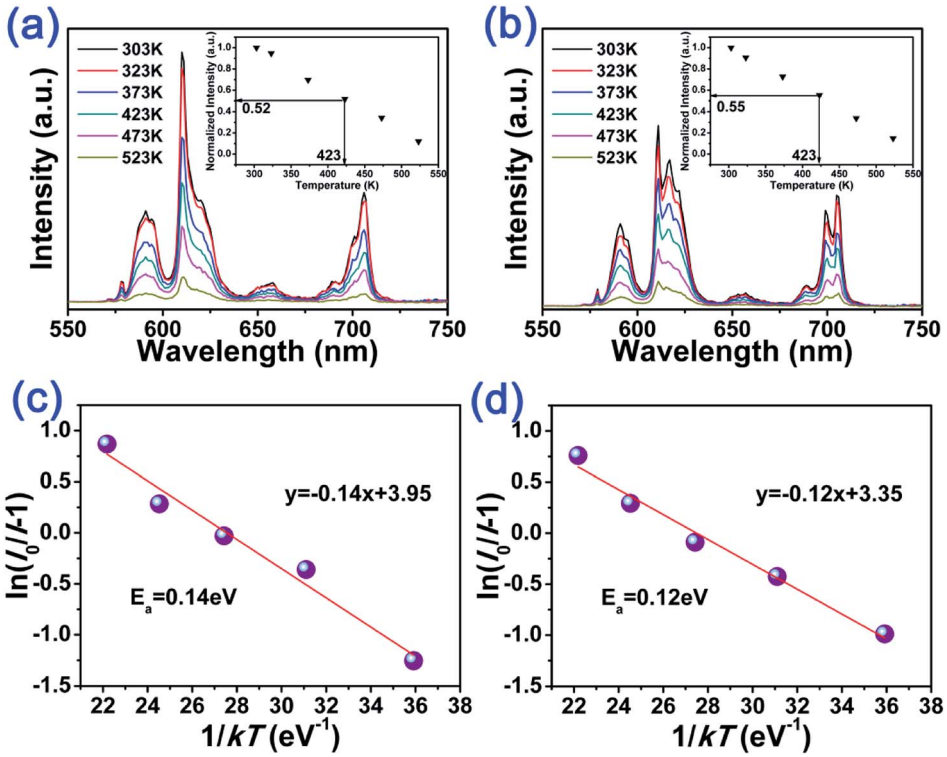

Fig. 3 Temperature-dependent PL spectra of (a) BEB:0.3Lu^{3+} and (b) BEB phosphors excited at 395 nm (The insets show normalized PL intensity as a function of temperature.). The plots of $\ln(I_0/I - 1)$ *versus* $1/kT$ and the calculated activation energy (E_a) for (c) BEB:0.3Lu^{3+} and (d) BEB phosphors.

determined to be 1.84, 1.95, 2.19, 2.18, 2.08, and 1.68 ms for $x =$ 0, 0.1, 0.3, 0.5, 0.7, and 0.9. Obviously, with increasing Lu^{3+} ions concentration, the lifetimes of Eu^{3+} ions rose and reached a maximum peak when $x = 0.3$, then dropped rashly. The reason of this phenomenon can be attributed to the fast non-radiative energy transfer between the adjacent Eu^{3+} ions: Lu^{3+} ions substituted a part of Eu^{3+} ions can alleviate the probability of non-radiative energy transfer by enlarging the distance of Eu^{3+}–Eu^{3+}. However, the loss of luminous centers (Eu^{3+} ions) result in the decline on Eu^{3+} lifetimes,[59] which can explain the decline trend after $x > 0.3$.

In order to investigate the effect on thermal stability of BEB:xLu^{3+} phosphors, we measured the temperature-dependent emission spectra of BEB:xLu^{3+} phosphors. The temperature dependent PL spectra of representative BEB and BEB:0.3Lu^{3+} phosphors were shown in Fig. 3. As shown in the Fig. 3(a) and (b), the emission intensities at 423 K remained about 55% and 52% of that initial intensities at 303 K for BEB and BEB:0.3Lu^{3+} phosphors. Moreover, the values of other phosphors were within a range of 50% to 55%, demonstrating that BEB:Lu^{3+} phosphors possess good thermal stability.

To better understand the thermal effect on the PL intensity of the phosphors, the activation energy was calculated according to the modified Arrhenius equation, which can be used to fit the thermal quenching data for activation energy calculation:[20,23,60]

$$\ln\left[\left(\frac{I_T}{I_0}\right) - 1\right] = -\frac{E_a}{kT} + \ln C \quad (3)$$

in which I_0 is the initial emission intensity, I_T is the intensity at temperature T, E_a is the activation energy, C is a constant for a certain host and k is the Boltzmann constant, respectively. Fig. 3(c) and (d) show the plot of $\ln[(I_0/I) - 1]$ *vs.* $1/kT$, and the experimental data can be linear fitted with slopes of -0.14 and -0.12 for BEB:0.3Lu^{3+} and BEB phosphors, respectively. Thus the activation energy of thermal quenching for BEB:0.3Lu^{3+} was around 0.14 eV.

In order to further investigate the luminescence performance of BEB:xLu^{3+} phosphors, we measured their IQEs. The IQEs of BEB:xLu^{3+} were calculated by using the following formula:[61]

$$\eta_{IQE} = \frac{\int L_s}{\int E_R - \int E_S} \quad (4)$$

where L_s is the emission spectrum of the sample, E_S and E_R represent the integrated intensities of PLE spectra of BEB:Lu^{3+} phosphors and $BaSO_4$ powder, respectively.[36] Under a excitation at 395 nm, the IQEs value of BEB:xLu^{3+} phosphors were calculated to be 83%, 84%, 87%, 75%, 66% and 57% for $x = 0$, 0.1, 0.3, 0.5, 0.7, and 0.9. Therefore, doping appropriate Lu^{3+} ions in BEB can improve its IQE (the IQEs of representative BEB and BEB:0.3Lu^{3+} phosphors were described at Fig. 4(a) and Fig. 4(b) respectively). The high IQE value indicated that the BEB:0.3Lu^{3+} would be a potential red phosphor candidate.

Open Access Article. Published on 02 October 2018. Downloaded on 2/10/2026 8:09:48 AM.
This article is licensed under a Creative Commons Attribution-NonCommercial 3.0 Unported Licence.

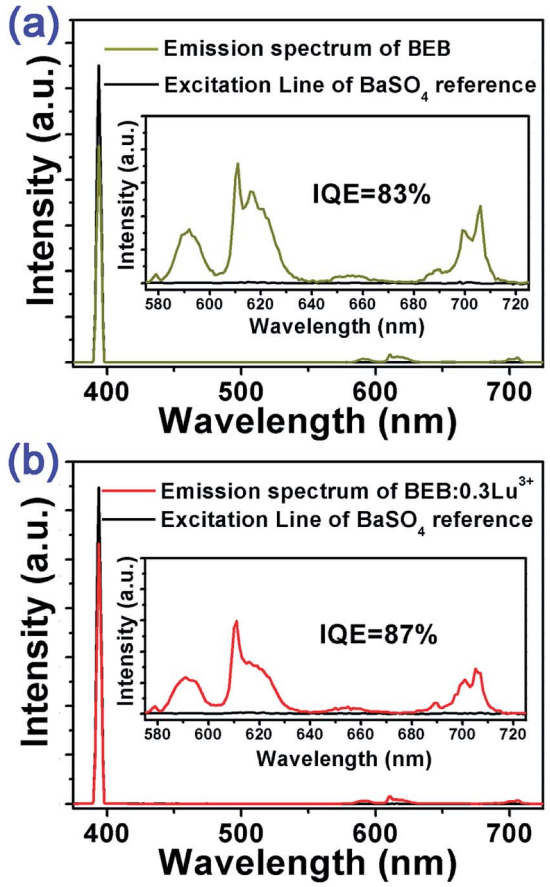

Fig. 4 Excitation line of $BaSO_4$ and the PL spectrum of (a) BEB phosphor and (b) BEB:0.3Lu^{3+} phosphor collected using an integrating sphere.

Compared with the commercial red phosphor $Y_2O_2S:Eu^{3+}$, BEB:0.3Lu^{3+} showed better performance under 395 nm excitation. As shown in Fig. 5, the BEB:0.3Lu^{3+} phosphor spanned more red region than $Y_2O_2S:Eu^{3+}$ phosphor, and the integrated emission intensity of BEB:0.3Lu^{3+} was about 3.25 times higher than that of $Y_2O_2S:Eu^{3+}$. In addition, we also calculated the color purity of BEB:0.3Lu^{3+} phosphor by using the following formula:[62]

$$\text{Color purity} = \frac{\sqrt{(x_s - x_i)^2 + (y_s - y_i)^2}}{\sqrt{(x_d - x_i)^2 + (y_d - y_i)^2}} \times 100\% \quad (5)$$

where (x_s, y_s) are the coordinates of sample point, (x_d, y_d) are the coordinates of the dominant wavelength, and (x_i, y_i) are the coordinates of the illuminant point.[63] For BEB:0.3Lu^{3+} phosphor, we took $(x_d, y_d) = (0.669, 0.331)$ for the dominant wavelength at 611 nm and $(x_i, y_i) = (0.310, 0.316)$ for the CIE illuminant point. The color purity of the BEB:0.3Lu^{3+} phosphor was found to be 91.4%, which is better than that of the commercial $Y_2O_2S:Eu^{3+}$ red phosphor ($x = 0.622$, $y = 0.351$; 87.2%).[64,65] These results demonstrated that BEB:0.3Lu^{3+} red phosphor may have much potential application for WLEDs.

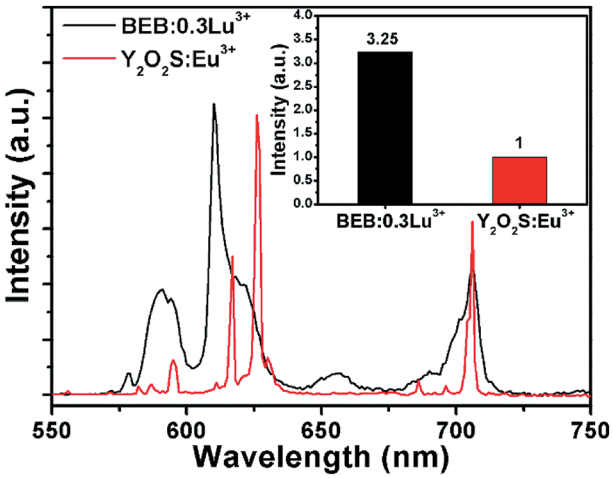

Fig. 5 Comparison of PL spectra of BEB:0.3Lu^{3+} and $Y_2O_2S:Eu^{3+}$ phosphors under 395 nm excitation.

Electroluminescence properties of fabricated WLED device

In order to evaluate the potential application of BEB:0.3Lu^{3+} phosphor, a warm WLED device was fabricated by the combination of a NUV chip (395 nm) with commercial blue BAM:Eu^{2+}, commercial green $(Ba,Sr)_2SiO_4:Eu^{2+}$ as well as red BEB:0.3Lu^{3+} phosphors.[66,67] The electroluminescence (EL) spectrum of this WLED was shown in Fig. 6. The bright warm white light can be seen in the inset of Fig. 6. Under a 20 mA current, the luminous efficacy, CCT, CRI, and CIE chromaticity coordinate of this WLED device were determined to be 15.98 lm W^{-1}, 3377 K, 84.7, and (0.412, 0.393) respectively. The above values of this WLED device under various currents were also measured (see Table 2). There was a little variation of the chromaticity coordinates, which confirmed the stable white light output in the device. Furthermore, the values of luminous efficacy, CCT and CRI were

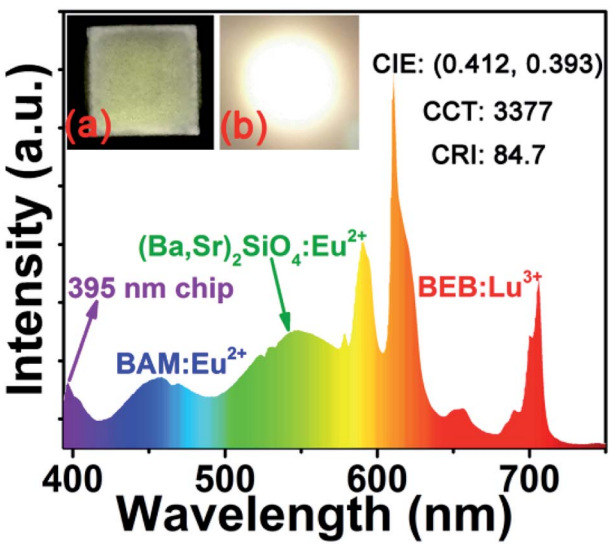

Fig. 6 EL spectrum of the fabricated WLED device combined by a 395 nm NUV chip and BAM:Eu^{2+}, $(Ba,Sr)_2SiO_4:Eu^{2+}$ and BEB:0.3Lu^{3+} phosphors driven by 20 mA current.

This journal is © The Royal Society of Chemistry 2018

Open Access Article. Published on 02 October 2018. Downloaded on 2/10/2026 8:09:48 AM.
This article is licensed under a Creative Commons Attribution-NonCommercial 3.0 Unported Licence.

Table 2 The corresponding CCT, CRI, CIE chromaticity coordinates (x, y), and luminous efficacy of the WLED device under different current

Current (mA)	CCT (K)	CRI	(x, y)	Luminous efficacy (lm W^{-1})
20	3377	84.7	(0.412, 0.393)	15.98
60	3298	84.8	(0.415, 0.392)	17.22
120	3251	84.8	(0.417, 0.391)	18.61
180	3216	84.8	(0.418, 0.390)	20.08
240	3189	84.7	(0.410, 0.390)	21.80
300	3164	84.6	(0.421, 0.389)	23.60

improved by applying higher currents. Under 300 mA current, luminous efficacy, corresponding CCT and CRI can be improved to 23.60 lm W^{-1}, 3164 K and 84.6. These results suggest that the as-synthesized red-emitting BEB:0.3Lu^{3+} would be a potential candidate red phosphor for WLEDs.

Conclusions

A series of Lu^{3+} doped BEB red phosphors were successfully synthesized by a high-temperature solid-state reaction method. Through investigating photoluminescence properties of these phosphors, we found that substituting partially of Eu^{3+} ions by Lu^{3+} ions can improve BEB's emission intensity and IQE. The optimal phosphor, BEB:0.3Lu^{3+}, possessed high IQE (87%), good color purity (91.4%) and good thermal stability (the integrated emission intensity at 423 K was around 52% of that at 303 K). By using commercial BAM:Eu^{2+} blue phosphor, commercial $(Ba,Sr)_2SiO_4$:Eu^{2+} green phosphor, as-prepared BEB:0.3Lu^{3+} red phosphor and a 395 nm NUV chip, a prototype warm white LED device was fabricated, which showed good color rendering index (CRI = 84.7) and low correlated color temperature (CCT = 3377 K). The results indicate BEB:0.3Eu^{3+} can be used as a potential red phosphor for warm WLED.

Conflicts of interest

There are no conflicts to declare.

Acknowledgements

This work was supported by the National Natural Science Foundation of China (No. 51502190), the Program for the Outstanding Innovative Teams of Higher Learning Institutions of Shanxi, and the Open Fund of the State Key Laboratory of Luminescent Materials and Devices (South China University of Technology, No. 2017-skllmd-01).

Notes and references

1 P. Du, L. Luo, X. Huang and J. S. Yu, *J. Colloid Interface Sci.*, 2018, **514**, 172–181.
2 X. Huang and H. Guo, *Dyes Pigm.*, 2018, **152**, 36–42.
3 X. Huang, B. Li, P. Du, H. Guo, R. Cao, J. S. Yu, K. Wang and X. W. Sun, *Dyes Pigm.*, 2018, **151**, 202–210.
4 X. Huang, J. Liang, B. Li, L. Sun and J. Lin, *Opt. Lett.*, 2018, **43**, 3305–3308.
5 X. Y. Huang, *J. Alloys Compd.*, 2017, **690**, 356–359.
6 P. Du, X. Huang and J. S. Yu, *Inorg. Chem. Front.*, 2017, **4**, 1987–1995.
7 P. Du, X. Huang and J. S. Yu, *Chem. Eng. J.*, 2018, **337**, 91–100.
8 X. Huang, S. Han, W. Huang and X. Liu, *Chem. Soc. Rev.*, 2013, **44**, 173–201.
9 G. Li, J. Chen, Z. Mao, W. Song, T. Sun and D. Wang, *Ceram. Int.*, 2016, **42**, 1756–1761.
10 Y. Liang, H. M. Noh, W. Ran, S. H. Park, B. C. Choi, J. H. Jeong and K. H. Kim, *J. Alloys Compd.*, 2017, **716**, 56–64.
11 X. Qiao, J. Xin, X. Nie, J. Xu, S. Qi and Z. Jiang, *Dyes Pigm.*, 2017, **143**, 103–111.
12 W. G. Liu, X. J. Wang, J. G. Li, Q. Zhu, X. D. Li and X. D. Sun, *Ceram. Int.*, 2017, **43**, 15107–15114.
13 L. Li, W. J. Wang, Y. Pan, Y. H. Zhu, X. G. Liu, H. M. Noh, B. K. Moon, B. C. Choi and J. H. Jeong, *RSC Adv.*, 2018, **8**, 1191–1202.
14 W. Li, J. Wang, H. Zhang, Y. Liu, B. Lei, J. Zhuang, J. Cui, M. Peng and Y. Zhu, *RSC Adv.*, 2016, **6**, 33076–33082.
15 S. Wang, Q. Sun, B. Li, H. Guo and X. Huang, *Dyes Pigm.*, 2018, **157**, 314–320.
16 X. Huang, *Nat. Photonics*, 2014, **8**, 748–749.
17 N. Guo, Y. C. Jia, W. Lu, W. Z. Lv, Q. Zhao, M. M. Jiao, B. Q. Shao and H. P. You, *Dalton Trans.*, 2013, **42**, 5649–5654.
18 R. Cao, C. Liao, F. Xiao, G. Zheng, W. Hu, Y. Guo and Y. Ye, *Dyes Pigm.*, 2018, **149**, 574–580.
19 Y. C. Chang, C. H. Liang, S. A. Yan and Y. S. Chang, *J. Phys. Chem. C*, 2010, **114**, 3645–3652.
20 S. Choi, Y. J. Yun, S. J. Kim and H. K. Jung, *Opt. Lett.*, 2013, **38**, 1346–1348.
21 B. Li, S. Wang, Q. Sun, C. Lu, H. Guo and X. Huang, *Dyes Pigm.*, 2018, **154**, 252–256.
22 X. Y. Huang, B. Li and H. Guo, *J. Alloys Compd.*, 2017, **695**, 2773–2780.
23 H. Guo, X. Huang and Y. Zeng, *J. Alloys Compd.*, 2018, **741**, 300–306.
24 Y. Liu, H. Zuo, J. Li, X. Shi, S. Ma, M. Zhao, K. Zhang and C. Wang, *Ceram. Int.*, 2016, **42**, 7781–7786.
25 Y. R. Wang, X. H. Liu, L. D. Jing and P. F. Niu, *Ceram. Int.*, 2016, **42**, 13004–13010.
26 R. Cao, T. Fu, Y. Cao, H. Ao, S. Guo and G. Zheng, *Mater. Lett.*, 2015, **155**, 68–70.
27 P. Du and J. S. Yu, *Dyes Pigm.*, 2017, **147**, 16–23.
28 H. X. Guan, Y. H. Song, P. C. Ma, M. Q. Chang, J. Chen, Y. X. Wang, B. Yuan and H. F. Zou, *RSC Adv.*, 2016, **6**, 53444–53453.
29 X. Huang, H. Guo and B. Li, *J. Alloys Compd.*, 2017, **720**, 29–38.
30 Y. Pan, W. Wang, Y. Zhu, H. Xu, L. Zhou, H. M. Noh, J. H. Jeong, X. Liu and L. Li, *RSC Adv.*, 2018, **8**, 23981–23989.
31 A. K. Parchur and R. S. Ningthoujam, *RSC Adv.*, 2012, **2**, 10859.
32 G. Jyothi and K. G. Gopchandran, *Dyes Pigm.*, 2018, **149**, 531–542.

Open Access Article. Published on 02 October 2018. Downloaded on 2/10/2026 8:09:48 AM. This article is licensed under a Creative Commons Attribution-NonCommercial 3.0 Unported Licence.

33 M. Shang, C. Li and J. Lin, *Chem. Soc. Rev.*, 2014, **43**, 1372–1386.
34 M. Wen, H. Wu, X. Su, J. Lu, Z. Yang, X. Wu and S. Pan, *Dalton Trans.*, 2017, **46**, 4968–4974.
35 J. Zhao, C. F. Guo, T. Li, X. Y. Su, N. M. Zhang and J. Y. Chen, *Dyes Pigm.*, 2016, **132**, 159–166.
36 J. Zhong, D. Chen, H. Xu, W. Zhao, J. Sun and Z. Ji, *J. Alloys Compd.*, 2017, **695**, 311–318.
37 B. Li, X. Huang, H. Guo and Y. Zeng, *Dyes Pigm.*, 2018, **150**, 67–72.
38 R. J. Yu, S. L. Zhong, N. Xue, H. J. Li and H. L. Ma, *Dalton Trans.*, 2014, **43**, 10969–10976.
39 V. Jubera, J. P. Chaminade, A. Garcia, F. Guillen and C. Fouassier, *J. Lumin.*, 2003, **101**, 1–10.
40 J. T. Ingle, R. P. Sonekar, S. K. Omanwar, Y. Wang and L. Zhao, *Solid State Sci.*, 2014, **33**, 19–24.
41 X. G. Zhang, Y. B. Chen, S. W. Zeng, L. Y. Zhou, J. X. Shi and M. L. Gong, *Ceram. Int.*, 2014, **40**, 14537–14541.
42 J. R. Cox, D. A. Keszler and J. Huang, *Chem. Mater.*, 1994, **6**, 2008–2013.
43 B. Howe and A. L. Diaz, *J. Lumin.*, 2004, **109**, 51–59.
44 B. H. Lee, H. G. Jeong and K. S. Sohn, *J. Electrochem. Soc.*, 2010, **157**, J227–J232.
45 R. D. Shannon, *Acta Crystallogr., Sect. A: Cryst. Phys., Diffr., Theor. Gen. Crystallogr.*, 1976, **32**, 751–767.
46 X. Qiao and H. J. Seo, *J. Alloys Compd.*, 2015, **637**, 504–508.
47 Y. Pan, W. Wang, L. Zhou, H. Xu, Q. Xia, L. Liu, X. Liu and L. Li, *Ceram. Int.*, 2017, **43**, 13089–13093.
48 L. Li, W. X. Chang, W. Y. Chen, Z. S. Feng, C. L. Zhao, P. F. Jiang, Y. J. Wang, X. J. Zhou and A. Suchocki, *Ceram. Int.*, 2017, **43**, 2720–2729.
49 H. Feng, Y. Yang and X. Wang, *Ceram. Int.*, 2014, **40**, 10115–10118.
50 X. Y. Huang and H. Guo, *Dyes Pigm.*, 2018, **154**, 82–86.
51 X. G. Zhang, Z. P. Zhu, Z. Y. Guo, F. W. Mo and Z. C. Wu, *Dyes Pigm.*, 2018, **156**, 67–73.
52 S. Zhang, P. Zhang, X. Liu and Z. Yang, *Ceram. Int.*, 2018, **44**, 15622–15626.
53 L. Zhang, B. Sun, C. Shao, F. Zhen, S. Wei, W. Bu, Q. Yao, Z. Jiang and H. Chen, *Ceram. Int.*, 2018, **44**, 17305–17312.
54 D. Qin and W. Tang, *RSC Adv.*, 2016, **6**, 45376–45385.
55 D. Qin and W. J. Tang, *RSC Adv.*, 2017, **7**, 2494–2502.
56 Y. Zhang, X. J. Zhang, H. R. Zhang, L. L. Zheng, Y. A. Zeng, Y. Lin, Y. L. Liu and B. F. Lei, *RSC Adv.*, 2018, **8**, 3530–3535.
57 D. Pi, F. Wang, X. Fan, M. Wang and Y. Zhang, *Spectrochim. Acta, Part A*, 2005, **61**, 2455–2459.
58 D. Boyer, G. Bertrand and R. Mahiou, *J. Lumin.*, 2003, **104**, 229–237.
59 D. Q. Chen, Y. L. Yu, P. Huang, H. Lin, Z. F. Shan and Y. S. Wang, *Acta Mater.*, 2010, **58**, 3035–3041.
60 X. P. Fu, W. Lu, M. M. Jiao and H. P. You, *Inorg. Chem.*, 2016, **55**, 6107–6113.
61 X. Y. Huang, B. Li and H. Guo, *Ceram. Int.*, 2017, **43**, 10566–10571.
62 S. Saha, S. Das, U. K. Ghorai, N. Mazumder, D. Ganguly and K. K. Chattopadhyay, *J. Phys. Chem. C*, 2015, **119**, 16824–16835.
63 X. Y. Huang, B. Li, H. Guo and D. Q. Chen, *Dyes Pigm.*, 2017, **143**, 86–94.
64 X. Zhang, L. Zhou, Q. Pang and M. Gong, *RSC Adv.*, 2015, **5**, 54622–54628.
65 L. Wang, W. Guo, Y. Tian, P. Huang, Q. Shi and C. E. Cui, *Ceram. Int.*, 2016, **42**, 13648–13653.
66 X. Huang, S. Wang, B. Li, Q. Sun and H. Guo, *Opt. Lett.*, 2018, **43**, 1307–1310.
67 J. Liang, P. Du, H. Guo, L. Sun, B. Li and X. Huang, *Dyes Pigm.*, 2018, **157**, 40–46.

This journal is © The Royal Society of Chemistry 2018